

RSC Advances



This is an *Accepted Manuscript*, which has been through the Royal Society of Chemistry peer review process and has been accepted for publication.

Accepted Manuscripts are published online shortly after acceptance, before technical editing, formatting and proof reading. Using this free service, authors can make their results available to the community, in citable form, before we publish the edited article. This *Accepted Manuscript* will be replaced by the edited, formatted and paginated article as soon as this is available.

You can find more information about *Accepted Manuscripts* in the [Information for Authors](#).

Please note that technical editing may introduce minor changes to the text and/or graphics, which may alter content. The journal's standard [Terms & Conditions](#) and the [Ethical guidelines](#) still apply. In no event shall the Royal Society of Chemistry be held responsible for any errors or omissions in this *Accepted Manuscript* or any consequences arising from the use of any information it contains.

ARTICLE

Immunosuppressive nano-therapeutic micelles downregulate endothelial cell inflammation and immunogenicity

Cite this: DOI: 10.1039/x0xx00000x

Received 00th March 2015,
Accepted 00th April 2015

DOI: 10.1039/x0xx00000x

www.rsc.org/

Satish N. Nadig^{a,b,e,†}, Suraj K. Dixit^{c,d,†}, Natalie Levey^a, Scott Eskilsen^a, Kayla Miller^{c,d}, William Dennis^a, Carl Atkinson^{b,e,*}, and Ann-Marie Broome^{c,d,e,*}

In this study, we developed a stable, nontoxic novel micelle nanoparticle to attenuate responses of endothelial cell (EC) inflammation when subjected to oxidative stress, such as observed in organ transplantation. Targeted Rapamycin Micelles (TRaM) were synthesized using PEG-PE-amine and N-palmitoyl homocysteine (PHC) with further tailoring of the micelle using targeting peptides (cRGD) and labeling with far-red fluorescent dye for tracking during cellular uptake studies. Our results revealed that the TRaM was approximately 10 nm in diameter and underwent successful internalization in Human Umbilical Vein EC (HUVEC) lines. Uptake efficiency of TRaM nanoparticles was improved with the addition of a targeting moiety. In addition, our TRaM therapy was able to downregulate both mouse cardiac endothelial cell (MCEC) and HUVEC production and release of the pro-inflammatory cytokines, IL-6 and IL-8 in normal oxygen tension and hypoxic conditions. We were also able to demonstrate a dose-dependent uptake of TRaM therapy into biologic tissues *ex vivo*. Taken together, these data demonstrate the feasibility of targeted drug delivery in transplantation, which has the potential for conferring local immunosuppressive effects without systemic consequences while also dampening endothelial cell injury responses.

Introduction

Solid organ transplantation is a widely accepted therapy for end-stage organ disease. While survival rates have improved significantly over the past 10 years, organs are still lost due to chronic rejection. Modern immunosuppressive regimens have significantly reduced acute rejection episodes but have done little to stem the incidence of chronic rejection.¹ The donor organ undergoes a number of injurious insults prior to, and during the early post-operative phase that are thought to contribute to the later development of chronic rejection.^{2,3} One such insult is ischemia reperfusion injury (IRI).⁴ IRI is an unavoidable complication in the process of cardiac transplantation, with the donor heart rendered ischemic for prolonged periods prior to implantation into the recipient and subsequent reperfusion. These processes damage the cardiac graft via activation of innate immune mechanisms, and the severity of this early inflammation and injury is associated with the ferocity and intensity of a subsequent adaptive immune response.⁵⁻⁹ The mechanisms contributing to the development of IRI are complex and multifaceted, and the pathophysiology

of IRI is complex. Ischemia results in the expression of normally hidden antigens and of various mediators of inflammation.

Once reperfusion occurs, the access of inflammatory mediators sets off an inflammatory reaction in which neutrophils, platelets, cytokines, molecular oxygen and complement play important roles, and which culminates in necrotic and apoptotic tissue death. Central to the pathogenesis are the endothelial cells (EC). EC sit at the interface between the graft and recipient immune response and early insults to EC within an organ allograft result in irreparable damage to the graft itself in both the short and long-term.¹⁰

Elegant studies by Collard *et al.*, 2000 suggest that oxidative stress is a key factor in the initiation of an immunologic insult, with *in vitro* and *in vivo* studies demonstrating a role for the endothelium in activating the immune system after IRI.¹¹ The immunologic damage to the cells lining the vasculature of organ allografts are thought to set a cascade of events in motion which ultimately lead to inappropriate antigen presentation to lymphocytes primed to attack the foreign organ.¹² The oxidative stress of ischemic

injury on EC plays a major role in endothelial dysfunction and rapid development of vascular disease. The insults of oxidative stress are also mediated, in part, by signaling through the mammalian target of the rapamycin (mTOR) intracellular pathway, which can be abrogated by rapamycin blockade.¹³ Therapeutics are clinically available for the treatment of oxidative stress; given that the oxidative insult occurs almost immediately post-IRI, the therapeutic window is small in the non-transplant setting. However, the oxidative insult experienced in transplantation is controllable since the time of reperfusion is controlled surgically, thus providing a larger window for therapeutic intervention.¹¹ Currently, no therapeutics are utilized to control IRI or the initiation of an adaptive immune response at this early time point post-transplantation.

Conventional immunosuppression globally reduces the immunological response by dampening the entire immune system to protect the newly grafted organ. However, side effects such as infections, cancers, and metabolic derangements are among the list of complications that organ transplant recipients suffer while on the necessary organ saving immunosuppressant medications. Furthermore, these therapies have little impact on the cascade induced during IRI. While significant advancements have been made with the design and efficacy of newer immunosuppressive medications, such as rapamycin, many carry heightened systemic risk profiles.¹⁴ Therefore, a potential way to circumvent the systemic side effects of immunotherapeutics and protect the organ graft is to develop strategies to specifically deliver these medications *directly* to the endothelium of grafted tissues to reduce local injury, inflammation, allopresentation, and the harmful side effects associated with their systemic counterparts.

The use of targeted immunosuppressive delivery allows for focused release of the medication at a specified cell type within the organ and provides the potential for local organ allograft tolerance. Targeted nanoparticle (NP) therapy is a novel alternative to delivering these vital medications in the setting of transplantation.^{15, 16} Various nanotherapeutic carriers exist and include liposomes, spherical and cylindrical fullerenes, viral particles, and micelle-based carriers.¹⁷ Among the existing options, micelles provide the ability to package hydrophobic payloads within their core and maintain a small size.

Recently, NPs have shown promising advances in the medical field with respect to treatment and diagnosis.^{18, 19} Most significant applications include drug delivery, diagnostics, and cancer therapy. However, the use of NPs in transplantation is still an emerging concept and in its infancy with very few descriptions in the current literature.²⁰⁻²² The attraction of NPs is, in large part, attributed to their unique physiochemical properties, such as their small size, stability and the ability for tailoring with various functionalities. In addition, the large functional surface on a NP is able to attach biomarkers and proteins. In order to design an efficient and effective drug carrier, certain issues need to be addressed: (1) a tailored surface on the carrier to attach biomolecules for targeted delivery; (2) a biocompatible composition which can efficiently

encapsulate the hydrophobic drug; and (3) stimuli-induced (i.e., pH) disruption of the carrier agent for drug release in the desired environment. Micelles are the preferred choice of carrier as they fulfill these requirements.^{23, 24} Micelles can be altered on their exterior surface with functional moieties, such as ligands or peptides, to provide targeting capability. The inner micelle core can be used as a container for many hydrophobic drugs. Environmental-sensitive lipids that take advantage of pH (or temperature) can be used to formulate the micelle shell to provide responsive drug release. In addition, polyethylene glycol (PEG) can be incorporated in the micelle structure to ensure long-term circulation without non-specific adsorption.

In this study, we use a novel, pH-sensitive, targeted micelle NP (**Fig. 1a**) to attenuate responses of human EC inflammation and allopresentation when subjected to oxidative stress such as in the case of solid organ transplantation. These micelles are decorated with cyclic Arginine-Glycine-Aspartate (cRGD) moieties to facilitate targeting to integrin alpha v beta 3 ($\alpha v \beta 3$) on the EC and loaded with the immunosuppressive rapamycin. Rapamycin, a potent mTOR inhibitor, was selected due to its ability to not only inhibit T cell effector cell functions, but also protect the endothelium. Studies have shown that rapamycin can modulate the upregulation of vascular endothelial growth factor, thereby conferring a protective effect on vascular endothelium, while also successfully attenuating endothelial injury and transplant vasculopathy in a humanized mouse aortic interposition graft model.^{25,26} Further, rapamycin may impede the emigration of passenger leukocytes to lymphoid organs, confirming that the release of rapamycin at the level of the organ itself may prevent the early IRI induced injury and further blunt alloimmune responses.²⁷ In addition to rapamycin loading, micelles were also conjugated to near infrared (NIR) fluorophores for tracking studies. The characterization and classification of these novel Targeted Rapamycin Micelles (TRaM) devices set the stage for future experiments investigating therapeutics for both acute and chronic allograft rejection in the setting of solid organ transplantation

Results

We synthesized nanocarrier constructs for *in vitro* analysis, Rapamycin Micelles (RaM) and Arginine-Glycine-Aspartate (cRGD) Targeted Rapamycin Micelles (TRaM). These rapamycin containing micelles were synthesized using PEG-PE-amine and N-palmitoyl homocysteine (PHC) (**Fig. 1a**). Amine functionality on PEG-PE amine was utilized for further tailoring of the micelle with the targeting cyclic peptide arginine-glycine-aspartate (cRGD) moiety, and labeled with the fluorescent dye, Dylight 680, for tracking the micelle in *in vitro* cellular uptake studies. Our results reveal that RaM are relatively monodisperse and measure at $9.8 \text{ nm} \pm 1.2 \text{ nm}$ (PDI 0.1) in size (**Fig. 1b**). Conjugation of TRaM with cRGD peptide shifts the size of the nanocarriers to approximately $15.3 \text{ nm} \pm 2.3 \text{ nm}$ (PDI 0.03) in size. Using dynamic light scattering (DLS), size distribution was found to be identical to the instrumental response function corresponding to a

monodispersed sample, indicating that aggregation is negligible. It is noteworthy that the hydrodynamic value is expected to be larger than the actual diameter because of the counter-ion cloud contributions to particle mobility. UV-Vis spectra (Fig. 1c) of RaM and TRaM show rapamycin and Dylight 680 excitation at 270 nm and 680 nm, respectively,

demonstrating encapsulation and conjugation, respectively, of both components. The concentration of the encapsulated rapamycin is calculated using UV-Vis spectroscopy; each batch is purified and concentrated for consistency.

Stability of the NPs was evaluated over a 24 hours period. To mimic the physiologic environment, the NPs were

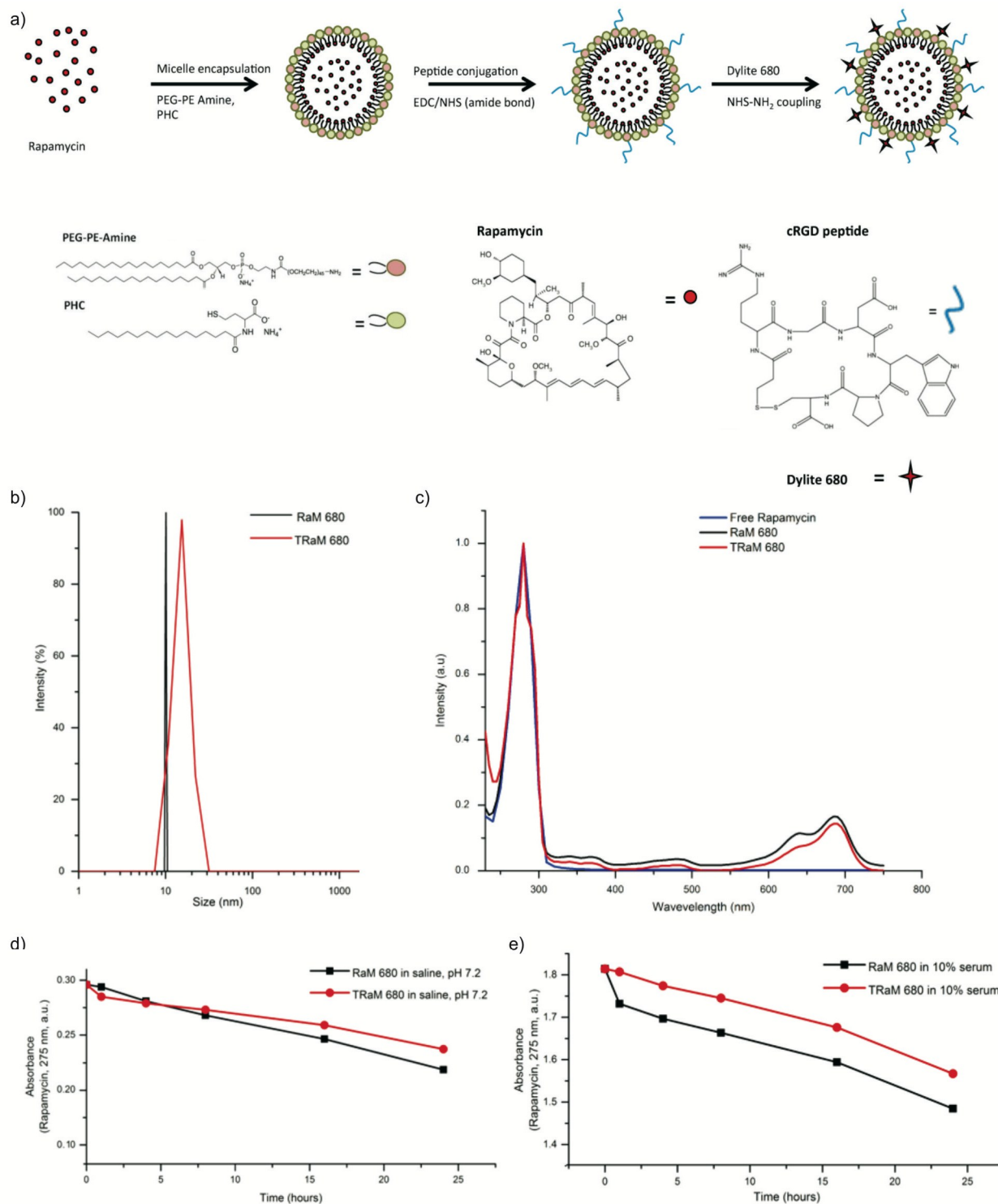


Fig. 1. Fabrication and characterization of rapamycin micelles. a) TRaMs are composed of rapamycin, NIR fluorophore (Dylight 680), and cRGD peptide targeting moiety for tracking and targeting purposes, respectively, b) Size calculation using DLS of RaM and TRaM demonstrates micelle sizes between 10-12 nm, c) UV-Vis spectroscopy of free rapamycin, RaM, and TRaM identifies rapamycin (275 nm) and Dylight 680 (692 nm). Concentration of each batch calculated based on the rapamycin peak. RaM and TRaM were assessed for stability over time in both phosphate buffered saline (d) and serum (e). Both NPs were able to maintain their composition over a 24 hours period.

suspended in saline (phosphate buffered saline (PBS), pH 7.2) and drug absorbance monitored (Fig. 1d). Both constructs were relatively stable over the 24 hours and did not show any significant aggregation of the drug (loss of absorbance at 275 nm of ~20-26%). The stability of these NPs was also tested in serum since the presence of lipids, amino acids, and proteins in the serum could contribute to NP instability (Fig. 1e). The NPs were slightly more stable than those suspended in saline over the same period with overall loss of absorbance at 275 nm of ~14-18%. These NP stability experiments confirmed the robust nature of the NPs for potential use in *in vivo* studies.

Rapamycin is encapsulated inside the hydrophobic micelle core, which reduces the interaction of the drug with the cellular environment. Encapsulation can potentially decrease cytotoxicity of the drug and subsequent side effects of parenchymal absorption. However, once the drug is delivered it must be released from its micelle package. PHC is a pH sensitive lipid that when incorporated within a micelle ruptures at an approximate pH of 5.0.^{28, 29} High absorbance of rapamycin is seen between a pH of 7.0 and 7.6 with less than 5% loss of fluorescence indicating that the TRaM remains intact in this physiologic range (Fig. 2). In contrast, RaM undergoes a 17.5% rupture within the same range, suggesting that the cyclic targeting moiety (cRGD) imparts some benefit in preventing rupture. These results further suggest that the NPs hold the rapamycin inside its core and resist rupture at physiologic pH. At a pH lower than 7 and higher than 8, the fluorescence intensity significantly decreases indicating the rupture of the micelle due to the pH sensitive lipid composition. Rapamycin is released from the micelle and the hydrophobic drug quickly aggregates within the hydrophilic solvent. Upon rupture, the free drug is then removed from the optical path of the excitation wavelength.

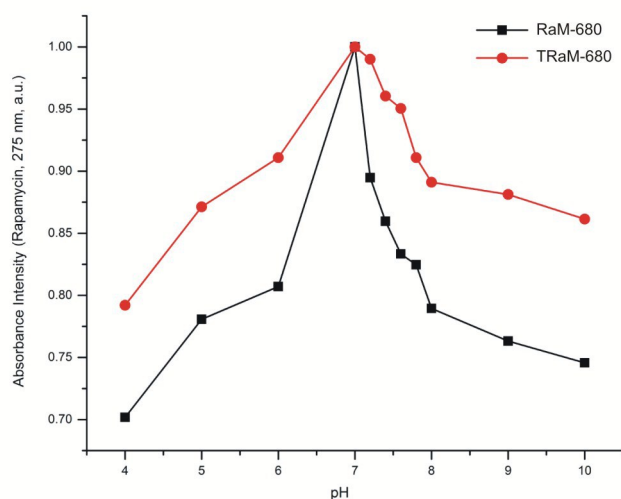


Fig. 2 pH-dependent release of encapsulated rapamycin. Absorbance of rapamycin (275 nm)-filled NPs is high between pH 7 and 7.6 and is lost outside of the physiologic range due to NP rupture.

Human umbilical vein ECs (HUVECs) and mouse cardiac endothelial cells (MCECs) were pre-treated for 6 hours with escalating doses of TRaM, RaM, empty micelles or free

rapamycin to assess cellular toxicity (Fig. 3). M-Per lysis of ECs was used as an assay control. After 6 hours of pre-treatment, a four hours MTS assay was performed as a colorimetric method for determining the number of viable, metabolically active cells. Nanoparticles with and without a therapeutic payload, along with free rapamycin showed no significant toxic effects on either EC lines (Fig. 3a, b). Additionally, at escalating doses, TRaM nanoparticle therapy exhibited no significant toxic effects on either MCECs (Fig 3c) or HUVECs (not shown). This lack of toxicity is not significantly different from that seen in free drug treated mouse and endothelial cells. Treatment with 3000 ng ml⁻¹ did induce toxicity; however, this was seen in both free drug and TRaM treated groups, for both cell lines.

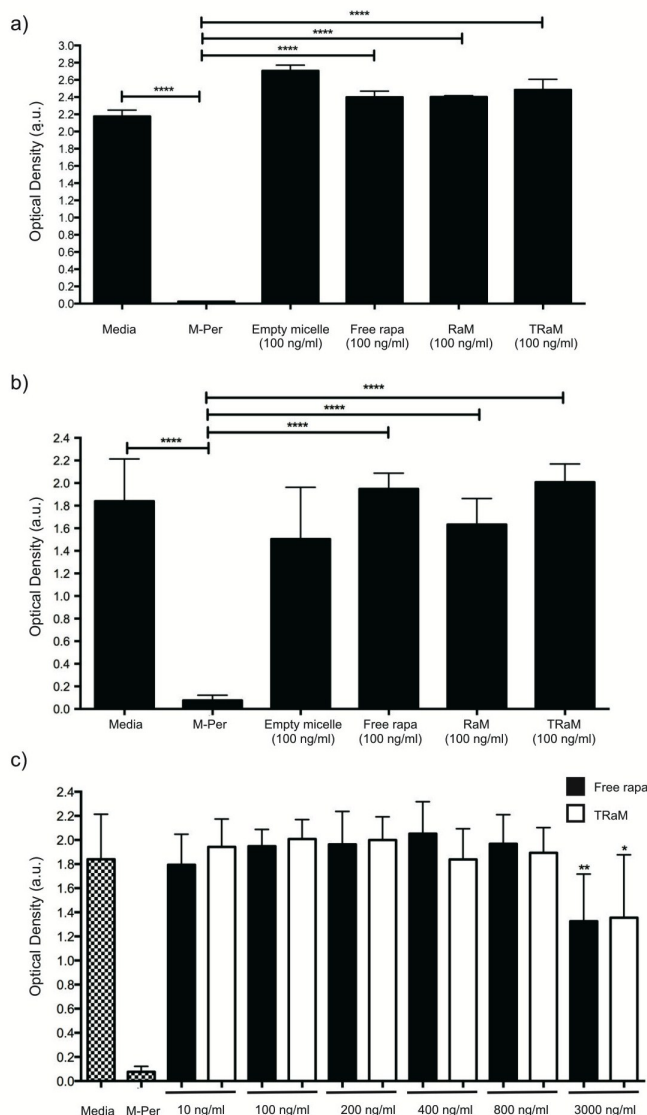


Fig. 3 TRaM impact on toxicity and cell viability. Standard MTS assays depicting the cell viability of a) HUVEC and b) MCEC cultured with a known toxic agent (M-per cell lysate), empty micelles, free drug, RaM, and TRaM for 6 hours. Treatment with empty micelle, free rapamycin, RaM or TRaM do not result in significant cell toxicity and death, c) MCEC cultured with increasing concentrations of free drug or TRaM do not show any significant cell death until 3000 ng ml⁻¹.

Micelles were functionalized with a cRGD peptide to target the $\alpha_V\beta_3$ integrin on EC surfaces to facilitate targeting and cellular uptake (Fig. 4a). To examine the intracellular uptake of our RaM and TRaM, human EC were incubated with these constructs for 6 and 24 hours periods and subsequently examined for micelle accumulation by visualization of the Dylight 680 fluorophore (red) on the micelles surface by confocal microscopy. Internalization was observed as early as 6

hours after incubation and internalization was concentration dependent (Fig. 4b). Targeting with cRGD significantly improved the micelle internalization by more than 50% as compared to untargeted RaM. $\alpha_V\beta_3$ integrin is well-characterized for its function related to angiogenesis as well as its expression on human EC. Additionally, cRGD has also been established as a prime candidate for targeting cells expressing $\alpha_V\beta_3$ integrin.³⁰ We confirmed the expression of $\alpha_V\beta_3$ integrin

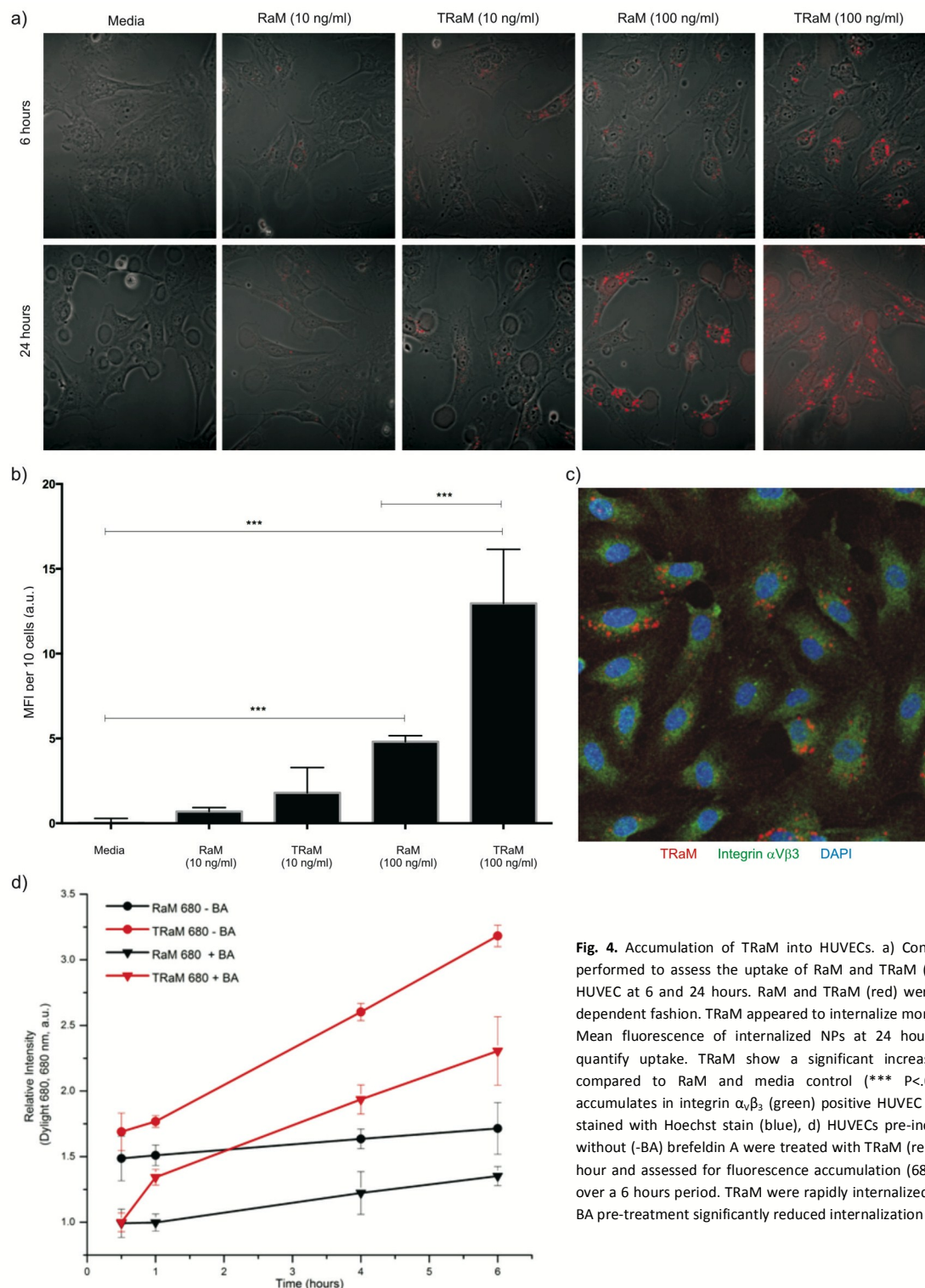


Fig. 4. Accumulation of TRaM into HUVECs. a) Confocal microscopy was performed to assess the uptake of RaM and TRaM (10 or 100 ng ml^{-1}) by HUVEC at 6 and 24 hours. RaM and TRaM (red) were taken up in a time-dependent fashion. TRaM appeared to internalize more rapidly than RaM, b) Mean fluorescence of internalized NPs at 24 hours was performed to quantify uptake. TRaM show a significant increase in intensity when compared to RaM and media control (***) $P < .001$, c) TRaM (red) accumulates in integrin $\alpha_V\beta_3$ (green) positive HUVEC after 24 hours. Nuclei stained with Hoechst stain (blue), d) HUVECs pre-incubated with (+BA) or without (-BA) brefeldin A were treated with TRaM (red) or RaM (black) for 1 hour and assessed for fluorescence accumulation (680 nm) within the cells over a 6 hours period. TRaM were rapidly internalized in the absence of BA. BA pre-treatment significantly reduced internalization of TRaM.

on the HUVEC cells used within these experiments and show in **Fig. 4c** the presence of TRaM within these $\alpha_v\beta_3$ integrin-expressing HUVECs.

To demonstrate that uptake of TRaM were predominantly due to endocytosis associated with the cRGD peptide and not diffusion of the micelles, HUVEC were treated with brefeldin A (BA), a fungal metabolite that reversibly interferes with intracellular transport and receptor cycling and examined for uptake (**Fig. 4d**). BA acts by inducing major structural changes in the morphology of endosomes, the trans-Golgi network, and lysosomes by causing the formation of an extensive tubular network and preventing new endosome formation.³¹ As seen

previously, significant fluorescence was observed when HUVEC were incubated with TRaM (-BA, 88% increase) over a 6 hours period. Fluorescence intensity increased by only 36% when HUVEC were treated with RaM (-BA). Pre-incubation with BA (+BA) decreased the relative fluorescence intensity of TRaM incubated cells by ~38% over time. RaM uptake was inhibited to a lesser extent with BA.

Given these data, we assessed the biologic efficacy of these novel targeted micelles. To determine the potential impact of local targeted delivery of rapamycin for later translation to organ transplantation, we performed *in vitro* culture experiments using a cell system to model the impact of

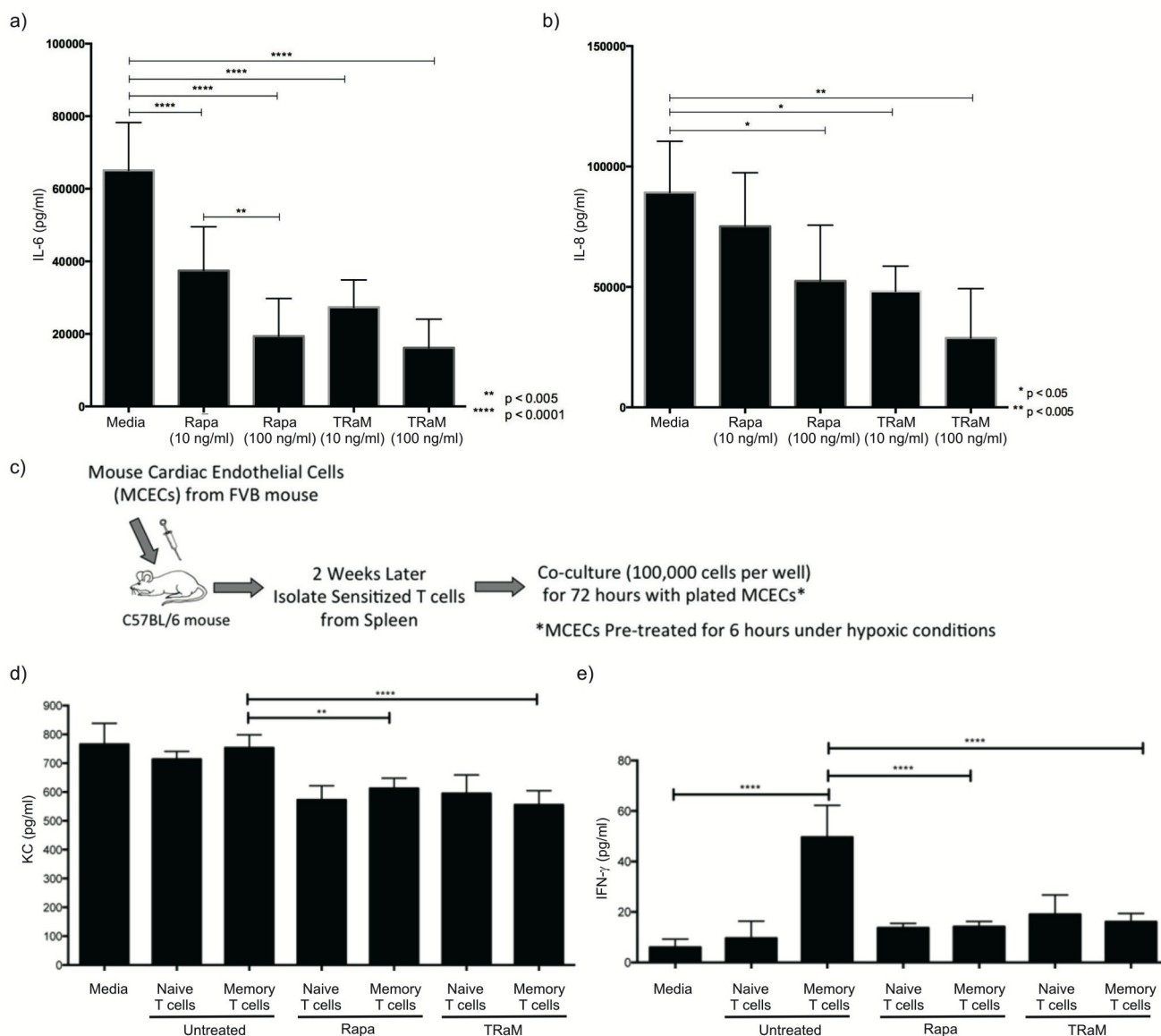


Fig. 5. Suppression of EC inflammation by TRaM internalization and release. ELISA were performed to assess the ability of TRaM to suppress biomarkers of EC inflammation. IL-6 (a) and IL-8 (b) were analyzed as markers of EC activation. HUVEC were subjected to oxidative stress with H_2O_2 and treated with either free rapamycin or TRaM (10 or 100 ng ml⁻¹). IL-6 and IL-8 were significantly suppressed by TRaM nanotherapy when compared to media alone, showing biological efficacy of targeted immunosuppressant nanotherapy *in vitro*, and had a similar effect as free rapamycin (IL-6: **** P<0.0001; ** p<0.005; IL-8: * p<0.05; **p<0.005). c) C57BL/6 mice were inoculated with MCEC from allogeneic FVB mice. T lymphocytes were then isolated from splenocytes 14 days later. Sensitized T cells were co-cultured with MCEC, which were either left untreated or pre-treated for 6 hours in a hypoxic chamber at 4°C with free rapamycin or TRaM to mimic cold storage ischemia, d) Production of mouse IL-8 (KC) by stimulated MCEC was significantly dampened by rapamycin and TRaM therapy (** p ≤ 0.01; **** p ≤ 0.0001), e) T cell production of IFN- γ was also significantly reduced in co-cultures when treated with free drug and TRaM therapy (***p ≤ 0.001).

reperfusion injury on EC activation and antigen presentation capacity (Fig. 5). The endothelium is the first site of donor organ interface with the recipient and is particularly susceptible to ischemia reperfusion injury. Further, the endothelium plays an important role in priming of the adaptive immune system, which contributes to the tempo and severity of the recipient rejection response. We treated human primary HUVEC that mimic the *in vivo* vascular target, with H₂O₂ in order to mimic the oxidative stress that occurs during the ischemia/reperfusion phase of solid organ transplantation (Fig. 5a, b). Cells were treated with 10 ng ml⁻¹ or 100 ng ml⁻¹ of free rapamycin or the TRaM constructs³². Oxidative injury to endothelial cells induces endothelial activation, which results in a pro-inflammatory phenotype that is characterized by the production and release of the pro-inflammatory cytokines, IL-6 (Fig. 5a) and IL-8 (Fig. 5b). H₂O₂ exposure significantly increased EC production of IL-6 and IL-8 and TRaM therapy significantly blunted this response.

Along with IRI, memory T cell responses remain a barrier to achieving tolerance in organ transplantation. To test the ability of TRaM to reduce cold storage, IR-induced endothelial activation, and memory T lymphocyte-induced injury, MCECs from FVB mice were used to inoculate allogeneic C57BL/6 mice. Sensitized T cells from the spleens of these mice were isolated using magnetic cell sorting 14 days later and co-cultured with MCEC in UW solution at 4°C in a hypoxic chamber with or without TRaM therapy (100 ng ml⁻¹). Efficacy of TRaM therapy was assessed by measuring mouse IL-8 (KC), a marker of EC activation, from MCEC and IFN-γ, a T cell cytokine, by T cells. As shown in Fig. 5, biomarkers of inflammation in a clinically relevant model of cold ischemia are significantly reduced by both EC and T cells when treated with TRaM therapy on par with the standard of care (Fig. 5c-e). These data suggest that targeted drug delivery demonstrates equivalent efficacy to standard therapy in the face of oxidative stress induced injury and can uniquely down regulate memory T cell responses in a novel, model of cold-storage hypoxia.

Finally, we examined whether encapsulated rapamycin would accumulate in aortic grafts soaked for 6 hours in cold UW solution containing increasing concentrations of TRaM (Fig. 6). Spectral analysis revealed uptake of TRaM and RaM in a dose-dependent fashion, beginning with as little as 500 ng ml⁻¹ in *ex vivo* aortas. Little micelle uptake was observed in aorta grafts incubated with RaM or empty micelles. The micelles remained intact over the 6 hours period as observed by fluorescence.

Discussion

Transplantation has become the modality of choice for the treatment of failed or failing organs. The field of transplantation has made tremendous strides over the last thirty years, in large part, due to more effective immunosuppressive medications rendering acute rejection episodes less frequent and less aggressive. In spite of these accomplishments, chronic rejection remains a leading cause of graft loss in the long term.³³

Currently, 90% of most solid organ transplants are functioning at one year, which is a tremendous leap from the one-year graft survival of approximately 60% three decades ago.³⁴⁻³⁶

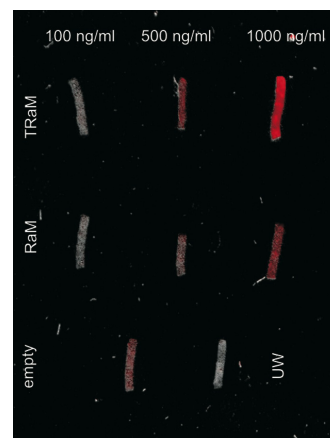


Fig. 6. Delivery of TRaM to aortic grafts with dose-dependent uptake. Aortas surgically removed from mice were incubated over 6 hours with TRaM (top), RaM (middle), empty micelles (bottom left), or cold UW solution (bottom right). The organs were imaged using *ex vivo* fluorescence imaging. Multispectral analysis was conducted to reveal fluorescence (680 nm) due only to intact micelles (red).

However, rates of long-term graft loss remain constant with only about 20% of heart transplants surviving 20 years or longer.^{36, 37} Translational research efforts have identified pathways and potential therapeutics that may allay the effects of chronic rejection in transplant recipients both experimentally and in early clinical trials.³⁸

Along with chronic rejection, transplant recipients continue to suffer the dire consequences of systemic immunosuppression. These medications, although a necessity, carry a host of serious and often fatal side-effects that range from new onset diabetes to lymphomas.³⁹ Certain immunosuppressants, such as rapamycin, inhibit the attacking T lymphocyte's ability to proliferate by halting cellular proliferation at the mTOR.⁴⁰ These mTOR inhibitors have proven to be more advantageous than standard calcineurin inhibitors in their ability to prevent the progression of vascular disease and endothelial dysfunction.²⁶ Rapamycin delivered systemically, or as part of a coated stent has been well established to slow the progression of smooth muscle cell proliferation inhibiting neointimal hyperplasia and arteriosclerosis within venous and arterial lumens.^{26, 41-43} Interestingly, rapamycin-releasing polymers have also been recently shown to reduce fibro-proliferative lesions in injury models of carotid arteries when delivered as a perivascular sheath.⁴⁴ Rapamycin, has also been touted as tolerogenic, as it has the potential ability to skew a transplant recipient's immunologic phenotype to one that is more advantageous to the grafted organ.³⁸ The synergy between mTOR inhibition and statin therapy, which many transplant recipients are prescribed, has also confirmed the presence of protective effects at the level of the endothelium in the combination's ability to protect EC from injury driven by the innate immune system.⁴⁵ Despite these physiologic and immunologic advantages, rapamycin is

seldom used clinically due to a significant side-effect profile.^{38, 46} Patient's taking rapamycin suffer from a spectrum of adverse consequences that includes, but is not limited to, metabolic derangements, intolerance to the medication, and impaired wound healing.⁴⁷

There is emerging and established evidence that immunoregulation may be beneficial at the local level of a graft itself and that rapamycin may blunt the trafficking ability of passenger leukocytes, which may allow for a more specific target for immunotherapeutics.^{27, 48, 49} Rapamycin NPs have been shown to dampen immune responses and provide modest prolongation of allografts when administered systemically.²¹ Although, the concept of targeted drug delivery has been the focus of investigative strategies in the oncologic literature, immunologists have yet to study the effects of triggered-released focused drug delivery in the setting of organ transplantation. Here, for the first time, we utilized a novel delivery method wherein an immunotherapeutic is encapsulated in a biologically inert NP and delivered to endothelium in a focused manner with a pH sensitive triggered-release mechanism. Together, these data suggest that the specific delivery of these pH sensitive, endothelial integrin cell-targeted NPs are able to blunt alloantigen presentation by HUVEC in an *in vitro* model of transplant IRI. The eventual goal of this novel therapy is to "pre-treat" donor organ endothelia by utilizing TRaM as an additive to hypothermic storage solutions. The rapamycin-coated vasculature would be hypothesized to minimize the harmful systemic side effects of traditional pharmacotherapies along with allowing for protection from the initial insults of organ ischemia and reperfusion.

The studies presented here represent the foundation for future applications of TRaM therapy either *ex vivo* or *in vivo*. The application of TRaM therapy would change the way we provide induction and maintenance immunosuppression to our transplant recipients. By delivering the drug in a targeted manner with focused release, the activation and initial immunologic insult may be blunted, which would allow for lower doses of induction therapy at the time of transplantation, and potential lower and less frequent doses of maintenance immunotherapy. The delivery of this device as an additive in standard perfusion and cold storage solution would serve as an initial step to clinical translation. Furthermore, this novel device may also serve as a platform for additional immunomodulating payloads as well as alternative targeting moieties. By delivering the drug in a targeted manner with focused release in the endothelium, the activation and initial immunologic insult may be blunted leading to an attenuation of the downstream immunologic and inflammatory insults seen in IRI.

We not only propose a novel application of standard immunosuppression, but also refine existing delivery methods to achieve drug-delivery to the endothelia of organ allografts for eventual use in solid organ transplantation. A continuous challenge in transplantation is balancing the anti-rejection effects of immunomodulating drugs with the inherent toxicities they inevitably incur. Therefore, using existing nanotechnology

with specific targeting to the endothelium of organs may be the ideal way to achieve operational tolerance, which is defined as immunosuppression to the organ while keeping the global immune system intact. EC line the vasculature in all solid organ transplants and are arguably the site of the initial immunologic insult in transplantation, which make them an ideal target for immunosuppressive delivery

Experimental methods

Cell Culture. Human Umbilical Vein Endothelial Cells (HUVEC), complete endothelial growth medium-2 (EGM-2) and bullet kit were purchased from Lonza (Walkersville, MD). Cells were grown and maintained in a humidified 37°C and 5% CO₂ atmosphere. Cells were expanded on T75 cm² polystyrene flasks to passage 5 and plated onto 6-well plates for experimental assays (Fischer Scientific, Pittsburgh, PA). MCEC, a normal mouse cardiac endothelial cell line from Cedarlane (Ontario, Canada), were cultured in Dulbecco's Modified Eagle Medium (DMEM) (Life Technologies, CA) supplemented with 10% fetal bovine serum (FBS) in a 37°C incubator with humidified room air and 5% CO₂.

Preparation of micelle encapsulated rapamycin. Micelle encapsulation of rapamycin (RaM) was carried out as described by Dubertret et al.⁵⁰ Typically, rapamycin was mixed with 2.5 mg amino-PEG-PE (1,2-diacyl-sn-glycero-3-phosphoethanolamine-N-[amino-poly(ethylene glycol)]) and 0.5 mg PHC (N-palmitoyl homocysteine (ammonium salt)), suspended in 1 ml of chloroform. The chloroform mixture was sonicated for 30 minutes at room temperature in a water bath. The solvent was evaporated in a vacuum oven at room temperature for 3 hours. Lipids were purchased from Avanti Polar Lipids (AL). The pellet obtained after evaporation was heated to 80°C and dissolved in nanopure water to produce amine-functionalized micelles. The micelle solution was sonicated for 1 hour in a water bath and filtered using a 0.2 µm syringe filter to remove aggregates. For the synthesis of TRaM, the RaM solution was used for peptide conjugation (1:1 ratio of carboxyl group on peptide to amine group on the micelles at 30% coverage of amines). 10 µl of cRGD (1 mg per 200 µl in DMSO) was added to 1 ml of MES buffer (pH 4.5) in separate scintillation vials followed by 4 µl EDC and 11 µl sulfo-NHS (10 mg per 100 µl in MES). After 15 minutes of incubation at room temperature, PBS (pH ~12) was added to bring the pH back to 7.5. The micelle solution was added to the peptide solution and incubated for 2 hours at room temperature. Excess peptide was removed using 10K MWCO ultracentrifugal device (Millipore, MD) at 4000 rpm for 15 minutes at 4°C. For dye labeling, 1 µl of NHS Dylight 680 (1 mg per 200 µl in DMSO) was added at a ratio covering 30% amine groups of the micelles to RaM and TRaM, respectively. The solution was incubated for 1 hour at room temperature. Excess dye was removed using 10K MWCO ultracentrifugal device at 4000 rpm for 15 minutes at 4°C.

Characterization of micelle encapsulated rapamycin. Dynamic Light Scattering (DLS) of micelles in aqueous

solution was performed on a ZetaPALS particle analyzer (Brookhaven Instruments, NY). The respective aqueous master solution was diluted and sonicated to prevent aggregation. The solution was filtered using a 0.2 μm syringe filter before taking the measurements. The concentrations of each micelle batch were determined by UV-Vis absorption using a Biotek microplate spectrophotometer (Winooski, VT). For pH change experiments, PBS buffers of pH 4 - 9 were prepared. RaM or TRaM-cRGD ($\sim 10^{-4}$ M) were placed in a 96 well plate. PBS buffers of increasing pH were added to respective wells. The wells were incubated for 4 hours. After 4 hours, UV-Vis measurements were recorded at 275 nm (rapamycin absorbance).

In vitro treatments with encapsulated rapamycin. Cells were plated at consistent densities of $1-2 \times 10^5$ cells per well and grown to confluence. A 1 mg mL^{-1} stock solution of rapamycin (Sigma-Aldrich, WI) and dimethyl sulfoxide (DMSO) was prepared and stored at 4°C . The stock solution was used to prepare free rapamycin solutions and NPs as described previously. Targeted NPs, untargeted NPs, and free rapamycin were diluted in EGM-2 media to 10 and 100 ng mL^{-1} concentrations. Cells were pre-incubated with 0.01% DMSO vehicle, EGM-2 media, free rapamycin, or NPs for 1 hour. Cells were washed two times with 0.02% Bovine Serum Albumin diluted in Hanks Balanced Salt Solution (HBSS/BSA wash solution). H_2O_2 (30% w/w; Sigma-Aldrich, MO) was diluted in HBSS/BSA wash solution ($250 \mu\text{M}$) and was applied immediately to designated wells. Following an 1 hour incubation, cells were washed with HBSS/BSA wash solution. Cells were then incubated in EGM-2 media for an additional 72 hours. Supernatants were then collected and cells were counted for further experimental analysis.

Confocal microscopy. For visualization studies of cellular internalization of NPs, HUVEC were plated on 35 mm glass dishes (MatTek Corp., MA) and grown to confluence. NP solutions were prepared as described previously. Growth medium was replaced by NP solutions (10 or 100 ng mL^{-1}) or EGM-2 vehicle. Cells were incubated for either 6 or 24 hours. After incubation, cells were washed with EGM-2 and fixed with (4% w/w) paraformaldehyde (Affymetrix, CA) at room temperature for 5 minutes. Cellular internalization of the Dylight 680-conjugated NPs was visualized using an Olympus Fluoview FV10i LIV Confocal Microscope (Olympus, NC), 60x objective. Mean fluorescence intensity calculated and analyzed by ImageJ (NIH). All fluorescence intensities were normalized to vehicle control images.

Inhibition of endocytosis. HUVEC cells were plated on 25x25 mm coverslips at a density of 30,000 cells per coverslip and maintained overnight in media at 37°C in an incubator supplied with 5% CO_2 . Twenty four hours after plating, one set of cells were treated with 250 μl of brefeldin A (BA) solution ($10 \mu\text{g mL}^{-1}$ in media) and were incubated for 1 hour (+BA). Another set of coverslips was left with 250 μl of media as -BA controls. For the +BA set of cells, the BA solution in media was replaced

with 250 μl of 500 nM RaM 680 or TRaM 680 solutions. The -BA cells were treated with 250 μl of 500 nM RaM 680 or TRaM 680 solutions. Both set of cells were incubated with the NPs for 0.5, 1, 4 and 6 hours respectively. After treatment, the cells were washed with media and then fixed with 4% paraformaldehyde for 10 minutes followed by three washes with PBS buffer. For staining of nuclei, cells were incubated with DAPI. Uptake and co-localization of NPs were visualized by fluorescence microscope using a Leica DM 4000B microscope (Leica Microsystems, IL). The images were analyzed using ImageJ (NIH, MA) software for relative normalized intensities for comparison analysis.

Cell sorting. Spleens were surgically removed from mice and splenocytes were isolated via cell straining. CD90.2 Microbeads (Miltenyi Biotec, CA) were used along with an autoMACS Pro Separator (Miltenyi Biotec, CA) to isolate T-cells from splenocytes to $>95\%$ purity. T cells were then co-cultured (at 100,000 cells per well) with rapamycin or TRaM pre-treated MCECs in 12 well plates at 4°C in a hypoxic chamber.

Hypoxic cold storage cell culture model. A modified cell culture model that simulates the IR process of heart transplantation was used as previously described^{8, 51}. Briefly, a confluent monolayer of MCECs underwent a period of simulated cold ischemia time (CIT) for 6 hours by replacing the DMEM containing 10% FBS with University of Wisconsin (UW; Bridge to Life, SC), a clinically used heart preservation solution, in a sealed hypoxic chamber filled with nitrogen at 4°C . After CIT, cells underwent 24 hours of simulated reperfusion by removing the preservation solution and reintroducing fresh DMEM containing 10% FBS, and then were incubated under normal culture conditions. To test the ability of free rapamycin and TRaM to reduce cold storage and ischemia reperfusion-induced endothelial activation, EC were stored in UW with or without free rapamycin or TRaM at 100 ng mL^{-1} . Efficacy was tested by measurement of supernatant mouse IL-8 (KC) by ELISA assay (BD Biosciences, CA) 24 hours post-reperfusion.

Animals. Animal experiments were performed according to Institutional Animal Care and Use Committee (IACUC) approved policies and guidelines at the Medical University of South Carolina (MUSC). The housing, feeding and care of animals used for these experiments were directed by veterinarians on staff at MUSC, trained and experienced in the proper care, handling and use of the mice. Research was conducted in compliance with the *Animal Welfare Act* and other federal statutes and regulations pertaining to animals and experiments involving animals, and adheres to principles stated in the *Guide for the Care and Use of Laboratory Animals*, NRC publication, 2011 edition.

Ex vivo fluorescence imaging. Mouse aortas were surgically removed and incubated with increasing concentrations of TRaM, RaM, empty micelles or UW solution. The organs were imaged at 0, 6 and 24 hours. Fluorescent multispectral images

were obtained using the Maestro *In Vivo* Imaging System (PerkinElmer, MA). Multispectral images were acquired under a constant exposure of 2000 ms with an orange filter acquisition setting of 630-850 nm in 2 nm increments. Multispectral images were unmixed into their component spectra (Dylight 680, autofluorescence, and background) and these component images were used to gain quantitative information in terms of average fluorescence intensity by creating regions of interest (ROIs) around the organs in the Dylight 680 component images.

Statistical analysis. All data is expressed as mean \pm SD. All data analysis was performed using GraphPad Prism software version 6 (La Jolla, CA) unless specified. Multiple variables were analyzed via analysis of variance techniques, p value <0.05 was considered statistically significant.

Conclusions

Targeted drug delivery represents the future of immunosuppressive therapy in transplantation. Currently, all immunosuppressive medication regimens are delivered systemically, which places recipients at risk for various downstream and often fatal side effects ranging from diabetes to cancer. Here, we show that targeted delivery is possible and, furthermore, may be used to pre-treat organs prior to the advent of implantation. Utilizing the cold storage ischemic time that inevitably occurs with all solid organ transplants as a time for therapy by using TRaM as an additive to standard *ex vivo* storage solutions allows for a greater potential of achieving tolerance in organ transplantation. Taken together, these data set the stage for future *in vivo* experiments utilizing clinically-relevant vascularized models of transplantation.

Acknowledgements

Portions of this work were supported by the South Carolina Clinical & Translational Research (SCTR) Institute, with an academic home at the University of South Carolina CTSA, NIH/CATS grant number UL1TR000062 (AMB and SNN) and the American Heart Association SDG 065100 (CA). The contents are solely the responsibility of the authors and do not necessarily represent the official views of the National Institutes of Health.

Notes

^a Department of Surgery, Division of Transplant, Medical University of South Carolina, 96 Jonathan Lucas Street, Charleston, SC 29425, USA. Fax: 01 843 792 8596; Tel: 01 843 792 8596; E-mail: nadign@muscu.edu.

^b Department of Microbiology and Immunology, Medical University of South Carolina, 173 Ashley Avenue, Charleston, SC 29425, USA. Fax: 01 843 792 2464; Tel: 01 843 792 1716; E-mail: atkinsoc@muscu.edu.

^c Department of Radiology & Radiological Science, Medical University of South Carolina, 68 President Street MSC 120, Charleston, SC 29425,

USA. Fax: 01 843 876 2469; Tel: 01 843 876 2481; E-mail: broomea@muscu.edu.

^d Center for Biomedical Imaging (CBI), Medical University of South Carolina, 68 President Street MSC 120, Charleston, SC 29425, USA. Fax: 01 843 876 2469; Tel: 01 843 876 2481; E-mail: broomea@muscu.edu.

^e South Carolina Investigators in Transplantation (SCIT), Medical University of South Carolina, 96 Jonathan Lucas Street, Charleston, SC 29425, USA. Fax: 01 843 792 8596; Tel: 01 843 792 3553; E-mail: nadign@muscu.edu.

† These authors contributed equally to this manuscript.

* Corresponding author

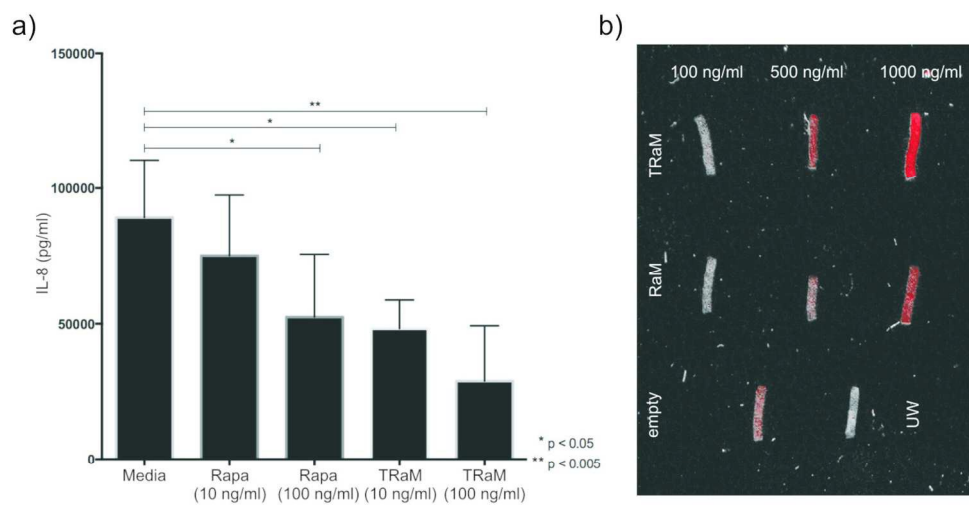
References

1. M. Boersema, H. Rienstra, M. van den Heuvel, H. van Goor, M. J. van Luyn, G. J. Navis, E. R. Popa and J. L. Hillebrands, *Transplantation*, 2009, 88, 1386-1392.
2. M. Wszola, A. Kwiatkowski, P. Domagala, A. Wirkowska, M. Bieniasz, P. Diuwe, K. Rafal, M. Durluk and A. Chmura, *Progr Transplant*, 2014, 24, 19-26.
3. D. K. de Vries, L. G. Wijermars, M. E. Reinders, J. H. Lindeman and A. F. Schaapherder, *Clinical transplantation*, 2013, 27, 799-808.
4. K. Miura, H. Sahara, M. Sekijima, A. Kawai, S. Waki, H. Nishimura, K. Setoyama, E. S. Clayman, A. Shimizu and K. Yamada, *Transplantation*, 2014, DOI: 10.1097/TP.0000000000000358.
5. N. C. Riedemann and P. A. Ward, *The American journal of pathology*, 2003, 162, 363-367.
6. C. Atkinson, S. He, K. Morris, F. Qiao, S. Casey, M. Goddard and S. Tomlinson, *J Immunol*, 2010, 185, 7007-7013.
7. G. H. Danton and W. D. Dietrich, *Journal of neuropathology and experimental neurology*, 2003, 62, 127-136.
8. W. Gao, J. Zhao, H. Kim, S. Xu, M. Chen, X. Bai, H. Toba, H. R. Cho, H. Zhang, S. Keshavjeel and M. Liu, *J Heart Lung Transplant*, 2014, 33, 309-315.
9. T. A. Khan, C. Bianchi, P. Voisine, J. Feng, J. Baker, M. Hart, M. Takahashi, G. Stahl and F. W. Sellke, *The Journal of thoracic and cardiovascular surgery*, 2004, 128, 602-608.
10. D. P. Basile, *Kidney international*, 2007, 72, 151-156.
11. C. D. Collard, A. Vakeva, M. A. Morrissey, A. Agah, S. A. Rollins, W. R. Reenstra, J. A. Buras, S. Meri and G. L. Stahl, *The American journal of pathology*, 2000, 156, 1549-1556.
12. G. Vassalli, A. Gallino, M. Weis, W. von Scheidt, L. Kappenberger, L. K. von Segesser and J. J. Goy, *European heart journal*, 2003, 24, 1180-1188.
13. A. G. Rajapakse, G. Yepuri, J. M. Carvas, S. Stein, C. M. Matter, I. Scerri, J. Ruffieux, J. P. Montani, X. F. Ming and Z. Yang, *PLoS one*, 2011, 6, e19237.
14. H. J. Eisen, *Current opinion in organ transplantation*, 2014, DOI: 10.1097/MOT.0000000000000119.
15. Y. Zhao, T. Zhang, S. Duan, N. M. Davies and M. L. Forrest, *Nanomedicine : nanotechnology, biology, and medicine*, 2014, DOI: 10.1016/j.nano.2014.02.015.
16. Z. Zhang, L. Xu, H. Chen and X. Li, *The Journal of pharmacy and pharmacology*, 2014, 66, 557-563.

17. D. M. Smith, J. K. Simon and J. R. Baker, Jr., *Nature reviews. Immunology*, 2013, 13, 592-605.
18. W. H. De Jong and P. J. Borm, *International journal of nanomedicine*, 2008, 3, 133-149.
19. J. Gao, H. Gu and B. Xu, *Accounts of Chemical Research*, 2009, 42, 1097-1107.
20. T. Gajanayake, R. Olariu, F. M. Leclere, A. Dhayani, Z. Yang, A. K. Bongoni, Y. Banz, M. A. Constantinescu, J. M. Karp, P. K. Vemula, R. Rieben and E. Vogelin, *Science translational medicine*, 2014, 6, 249ra110.
21. K. Y. Dane, C. Nembrini, A. A. Tomei, J. K. Eby, C. P. O'Neil, D. Velluto, M. A. Swartz, L. Inverardi and J. A. Hubbell, *Journal of controlled release : official journal of the Controlled Release Society*, 2011, 156, 154-160.
22. K. Goldmann, J. Hoffmann, S. Eckl, B. M. Spriewald and S. M. Ensminger, *Transplant immunology*, 2013, 28, 9-13.
23. K. Kataoka, A. Harada and Y. Nagasaki, *Advanced drug delivery reviews*, 2001, 47, 113-131.
24. N. Nasongkla, E. Bey, J. Ren, H. Ai, C. Khemtong, J. S. Guthi, S.-F. Chin, A. D. Sherry, D. A. Boothman and J. Gao, *Nano letters*, 2006, 6, 2427-2430.
25. C. Ponticelli, *Journal of nephrology*, 2004, 17, 762-768.
26. J. Hester, A. Schiopu, S. N. Nadig and K. J. Wood, *Am J Transplant*, 2012, 12, 2008-2016.
27. H. Hackstein, T. Taner, A. F. Zahorchak, A. E. Morelli, A. J. Logar, A. Gessner and A. W. Thomson, *Blood*, 2003, 101, 4457-4463.
28. J. Connor and L. Huang, *The Journal of cell biology*, 1985, 101, 582-589.
29. D. Collins, F. Maxfield and L. Huang, *Biochimica et biophysica acta*, 1989, 987, 47-55.
30. A. Adulnirath, S. W. Chung, J. Park, S. R. Hwang, J. Y. Kim, V. C. Yang, S. Y. Kim, H. T. Moon and Y. Byun, *Journal of controlled release : official journal of the Controlled Release Society*, 2012, 164, 8-16.
31. W. Hunziker, J. A. Whitney and I. Mellman, *Cell*, 1991, 67, 617-627.
32. Y. S. Kwon, H. S. Hong, J. C. Kim, J. S. Shin and Y. Son, *Investigative ophthalmology & visual science*, 2005, 46, 454-460.
33. B. J. Nankivell, R. J. Borrows, C. L. Fung, P. J. O'Connell, R. D. Allen and J. R. Chapman, *The New England journal of medicine*, 2003, 349, 2326-2333.
34. *The New England journal of medicine*, 1967, 277, 824-825.
35. J. M. Cecka, *Clinical transplants*, 2002, 1-20.
36. M. C. Alraies and P. Eckman, *Journal of thoracic disease*, 2014, 6, 1120-1128.
37. A. P. Monaco, *Transplantation*, 2003, 75, 13S-16S.
38. K. J. Wood, A. Bushell and J. Hester, *Nature reviews. Immunology*, 2012, 12, 417-430.
39. A. P. Monaco, *Transplant Proc*, 2004, 36, 227-231.
40. R. T. Abraham and G. J. Wiederrecht, *Annu Rev Immunol*, 1996, 14, 483-510.
41. H. J. Eisen, E. M. Tuzcu, R. Dorent, J. Kobashigawa, D. Mancini, H. A. Valentine-von Kaeppler, R. C. Starling, K. Sorensen, M. Hummel, J. M. Lind, K. H. Abeywickrama and P. Bernhardt, *The New England journal of medicine*, 2003, 349, 847-858.
42. J. Zou, X. Zhang, H. Yang, Y. Zhu, H. Ma and S. Wang, *Annals of vascular surgery*, 2011, 25, 538-546.
43. A. Haeri, S. Sadeghian, S. Rabbani, M. S. Anvari, A. Lavasanifar, M. Amini and S. Dadashzadeh, *International journal of pharmaceuticals*, 2013, 455, 320-330.
44. X. Yu, T. Takayama, S. A. Goel, X. Shi, Y. Zhou, K. C. Kent, W. L. Murphy and L. W. Guo, *Journal of controlled release : official journal of the Controlled Release Society*, 2014, 191, 47-53.
45. S. S. Hamdulay, B. Wang, D. Calay, A. P. Kiprianos, J. Cole, O. Dumont, N. Dryden, A. M. Randi, C. C. Thornton, F. Al-Rashed, C. Hoong, A. Shamsi, Z. Liu, V. R. Holla, J. J. Boyle, D. O. Haskard and J. C. Mason, *J Immunol*, 2014, 192, 4316-4327.
46. J. Verhave, A. Boucher, R. Dandavino, S. Collette, L. Senecal, M. J. Hebert, C. Girardin and H. Cardinal, *Clinical transplantation*, 2014, 28, 616-622.
47. D. R. Kuypers, *Drug safety : an international journal of medical toxicology and drug experience*, 2005, 28, 153-181.
48. M. Sandovici, L. E. Deelman, A. Benigni and R. H. Henning, *Advanced drug delivery reviews*, 2010, 62, 1358-1368.
49. T. Deuse, F. Blankenberg, M. Haddad, H. Reichenspurner, N. Phillips, R. C. Robbins and S. Schrepfer, *American journal of respiratory cell and molecular biology*, 2010, 43, 403-412.
50. B. Dubertret, P. Skourides, D. J. Norris, V. Noireaux, A. H. Brivanlou and A. Libchaber, *Science*, 2002, 298, 1759-1762.
51. J. A. Cardella, S. Keshavjee, E. Mourgeon, S. D. Cassivi, S. Fischer, N. Isowa, A. Slutsky and M. Liu, *Journal of applied physiology*, 2000, 89, 1553-1560.

TOC Abstract

Targeted micelles containing rapamycin (TRaM) suppressed immune response of IL-8 in oxidatively stressed human umbilical vein endothelial cells *in vitro* (a) and accumulated in aorta grafts for transplantation after 6 hours in cold perfusion solution (b).



Targeted micelles containing rapamycin (TRaM) suppressed immune response of IL-8 in oxidatively stressed human umbilical vein endothelial cells in vitro (a) and accumulated in aorta grafts for transplantation after 6 hours in cold perfusion solution (b).
177x101mm (300 x 300 DPI)